ISSN: 2319-6505

Available Online at http://journalijcar.org

International Journal of Current Advanced Research
Vol 5, Issue 9, pp 1205-1215, September 2016

RESEARCH ARTICLE

International Journal of Current Advanced Research

ISSN: 2319 - 6475

T4 LYSOZYME-ENGINEERED HUMAN CHEMOKINE RECEPTOR CCR5 MUTANTS EXHIBIT DIFFERING EFFECTS ON HIV-1 CO-RECEPTOR FUNCTION AND LIGAND BINDING

Qingwen Jin[1,2]., Qi Niu[3]., Wei Zhang[4]., LiandongZhao[5].,Hong Chen[3]., XingxiaWang[3]., QingchenXu[6]., Lin Ji[7],. Huijuan Wang[1]., GuanyuLi[8]., Xiaofan Yang[1] and Xiaohui Ji[1]*

[1]Department of Microbiology & Immunology, Nanjing Medical University,
#140 Hanzhong Road, Nanjing, Jiangsu Province, China
[2]Department of Neurology, Sir Run Run Hospital, Nanjing Medical University,
#109 LongmianDadao, Nanjing, Jiangsu province, China
Department of Neurology, The First Affiliated Hospital of Nanjing Medical University,
#300 Guangzhou Road, Nanjing, Jiangsu Province, China
4Drug Discovery Division, Southern Research Institute, #2000 Ninth Avenue South, Birmingham, Alabama, USA
[5]Department of Neurology, The Second Hospital of Huaian, #62 Huaihai South Road, Huaian, Jiangsu Province, China
[6]Department of Neurology, Nanjing First Hospital, #68 Changle Road, Nanjing, Jiangsu Province, China
[7]Department of Anesthesiology, The Third People's Hospital of Yancheng,
#75 Juchang Road, Yancheng, Jiangsu Province, China
[8]Department of Neurology, Mingji Hospital of Nanjing, Jiangsu Province,
#71 Riverside West Road, Nanjing, Jiangsu Province, China

A R T I C L E I N F O

Article History:

Received 29th June, 2016
Received in revised form 4th
July, 2016 Accepted 18th
August, 2016 Published online 23rdSeptember, 2016

Key words:

T4 lysozyme, CCR5, GPCR, HIV-1, recombinant protein

Abbreviations used: GPCR, G protein-coupled receptor; CCR5, CC chemokine receptor 5; RANTES, regulated on activation, normal T cell expressed and secreted; DMEM, Dulbecco's modified Eagle's medium; MIP-1α, macrophage inflammatory protein 1α; MIP-1β, macrophage inflammatory protein 1β.

A B S T R A C T

Background: The insertion of T4 lysozyme (T4L) to replace portions of G protein-coupled receptors has proved a successful approach to enhance protein stability and crystallization. However, T4L engineering alters the protein sequence and raises uncertainties regarding the details ofreceptor activationmodels that are based on the structures of receptor-T4L fusion proteins.

Methodology/Principal Findings: we generated six T4L-CCR5 variants containing a replacement at the first, second, or third intracellular loop or at different C-terminal regions and compared their functions. We demonstrated that only two of the constructs, T4L-CCR5-C352 and T4L-CCR5-ICL2, retain sufficient HIV-1 co-receptor function when expressed in HEK-293 cells. However, other constructs preserve the ability to bind and initiate signaling in response to chemokine CCL4 although T4L-CCR5-ICL1, T4L-CCR5-ICL3, and T4L-CCR5-C310 mutant receptors are defective in their abilities to activate G-proteins.

Conclusions/Significance: T4L replacement at the second intracellular loop retains the structural features of wild-type CCR5, whereas replacements at other positions may change the conformation of the N-terminus or the extracellular loops of CCR5.

INTRODUCTION

G protein-coupled receptors (GPCRs), which form the largest superfamily of drug targets, contain a 7-transmembrane structural feature and couple to G-proteins for signal transduction within the cell. Therefore, their three-dimensional structural and dynamic information is of great interest to researchers who aim to design effective drugs targeting GPCRs [1].In the past 5 years, protein engineering using T4 lysozyme (T4L) to improve the stability and solubility of GPCRs has been a major innovation that has contributed to most of the available structures of GPCRs. The creation of T4 lysozyme-containing fusions has facilitated the structural determination of the β2 adrenergic [2,3], A2a adenosine [4], dopamine D3 [5], CXCR4 chemokine [6], histamine H1 [7], lyso-phospholipid S1P [8], M2 and M3 muscarinic acetylcholine [9,10], and δ, κ, and μ-opioid [11,12,13] receptors. However, T4L engineering alters the protein sequence and raises uncertainties about the details ofreceptor activationmodels that are based on structures of receptor-T4L fusion proteins. All reported T4L-GPCR fusion structures that have been used for functional analysis retain the ability to bind ligands. Assays of G protein activation and HIV entry co-receptor activity [in the case of CXCR4 and CC chemokine receptor 5 (CCR5)] by T4L-GPCR fusion constructs have generally not been reported, because the chemokine receptor and viral entry co-receptor functionalities of these receptors are mutually independent.

CCR5 belongs to the GPCR superfamily and plays a crucial role in human immunodeficiency virus-1 (HIV-1) infection [14,15,16]. Moreover, it was found that individuals with genetic defects in CCR5 expression are relatively resistant to HIV-1 infection and do not exhibit obvious health problems [17,18,19]. This suggests that the CCR5 chemokine receptor is an ideal target for the treatment and prevention of HIV infection. The first CCR5-blocking drug, Maraviroc, was approved in 2007 [20]. Several CCR5 structural models have been reported in the literature [21,22,23,24]. Most of these are homology models built using the bovine rhodopsin structure as a template. Recently, an NMR CCR5 model was built based on the crystal structure of CXCR4 [25]. However, due to the low signal-to-noise ratio, unambiguous assignments could only be achieved for 21 residues within the CCR5 amino acid sequence. The quality of the NMR spectra of CCR5 is insufficient for structural analysis. More recently, a three-dimensional portrait of CCR5 attached to the HIV drug Maraviroc has been produced [26]. However, it is only one of the many snapshots of the structurally diverse CCR5 molecule. As a result, the association between the CCR5 structure and its function remains an enigma.

Here, we report the generation of six independent T4 lysozyme fusion CCR5 variants. We investigated the effects of T4L engineering in maintaining the structural conformation of the receptor, its ligand-binding properties, and signal transduction properties, as well as its ability to function as an HIV co-receptor. We found that only two constructs, T4L-CCR5-C352 andT4L-CCR5-ICL2, retain sufficient HIV-1 co-receptor function when expressed in HEK-293 cells. Other constructs preserve the ability to bind and initiate signaling in response to chemokine ligands. In addition, we observed thatT4Lreplacement at the third intracellular loop (T4L-CCR5-ICL3) can produce 10 milligrams of highly (>90%) purified recombinant protein from 1 liter of culture media using an *E.coli* expression system, a 10-fold increase in yield compared to that of other variants, including those with replacements at the first and second intracellular loops and at different C-terminal regions (T4L-CCR5-ICL1, T4L-CCR5-ICL3, T4L-CCR5-C352, T4L-CCR5-C333, and T4L-CCR5-C310). However, although all *E. coli*-produced recombinant T4L-CCR5 proteins could bind to CCL4 (MIP-1β) and affect cell migration *in vitro*, only the recombinant T4L-CCR5-C352 andT4L-CCR5-ICL2 proteins showed competitive inhibition activity in HIV-1 Env-mediated cell-cell fusion, indicating that they can act as novel inhibitors of HIV infection.

MATERIALS AND METHODS

Cells and other reagents

The HeLa, HEK-293, and THP1 cell lines were obtained from the American Type Culture Collection (Manassas, VA). The 3T3.T4 cell line was obtained from the NIH AIDS Reagent Program. All cell lines were maintained in Dulbecco's Modified Eagle Medium (Quality Biologicals, Gaithersburg, MD) containing 10% (vol/vol) fetal bovine serum (FBS), 2 mM glutamine, and 2 mM penicillin-streptomycin. Phycoerythrin (PE)-conjugated 2D7 and PE-conjugated 3A9 monoclonal antibodies were purchased from BD Biosciences (FranklinLakes, NJ). Monoclonal antibodies to CD4 and CCR5 were purchased from Santa Cruz Biotechnology, Inc. (Santa Cruz, CA). Mouse monoclonal His-tag antibody was purchased from Abcam (Cambridge, MA). [35S]GTPγS was obtained from GE Healthcare Bio-Sciences (Piscataway, NJ). Plasmids for human β-arrestin1, β-arrestin2, bovine G protein-coupled receptor kinase (GRK) 2 and GRK5 as well as T4 lysozyme WT vector were purchased from Addgene (Cambridge, MA). TAK-779 and Maraviroc were obtained from the NIH AIDS Reagent Program. Plasmids PcREV and pNL4-3.Luc+env were also obtained from the NIH AIDS Reagent Program. The PET-20b expression vector and the BL21-Gold (DE3) pLysS strain of *E. coli* were purchased from Stratagene (La Jolla, CA). Ni-nitrilotriacetic acid (NTA) histidine-binding beads were purchased from Sigma (St. Louis, MO). All detergents were purchased from Affymetrix (Santa Clara, CA). All other reagents (unless indicated) were from Sigma-Aldrich, (St. Louis, MO). Soluble CD4 and chemokine CCL5 were purchased from R&D Systems (Minneapolis, MN).

Generation of T4L-fused CCR5 constructs

Human CCR5 in the pSC-59 vector and T4 lysozyme WT vector were used as the starting templates for generating the T4L-fused CCR5 constructs. PCRs were carried out with the Faststart High Fidelity PCR System (Roche, Basel, Switzerland). The amplification protocol consisted of a 5-min denaturation at 94°C, followed by 30 cycles of denaturation at 94°C for 1 min, annealing at 55°C for 1 min, and extension at 72°C for 1 min. The amplified DNA strand was purified from an agarose gel using the PureLink Quick Gel extraction kit (Invitrogen, Carlsbad, CA). The entire CCR5-T4L cDNA without the stop codon was further subcloned into the pET-20b expression vector using the BamHI and XhoI restriction enzyme digestion sites, whereas CCR5-T4L cDNA with the stop codon was cloned into the pSC59-IRES-EGFP vector using the NheI and SacII restriction enzyme digestion sites. Both T4L-fused CCR5 constructs were confirmed by DNA sequencing (GENEWIZ, Inc., Suzhou, China).

Expression and purification of E. coli-expressed recombinant His-tagged T4L-fused CCR5 constructs

We transfected the recombinant pET-20b/T4L-CCR5 vector into gold BL21(DE3) pLysS*E. coli* host cells for optimal expression, as we have previously described [27]. Briefly, a single colony was inoculated into 5 ml of LB broth containing 200 g/ml ampicillin and 30 g/ml chloramphenicol, and shaken at 37°C overnight. After approximately 16 h of shaking, 5 ml of the inoculum was added to 1 liter of LB broth containing 200 g/ml ampicillin and 30 g/ml chloramphenicol. The 1-liter culture was shaken at 200 rpm and 37°C for approximately 5–8 h until an optical density at 600 nm (OD600) of 2.6 was achieved. The cultures were cooled on ice until the temperature dropped to 20°C. T4L-CCR5 expression was induced with a final concentration of 1 mM isopropyl β-D-thiogalacto-pyranoside (IPTG), and the cultures were shaken at 125 rpm at 20°C for 24 h. After being shaken, the cultures were centrifuged at 3,500 ×g and 4°C for 30 min. The supernatants were discarded, and the pellets were allowed to air-dry for 10 min before storing at –80°C until purification.

Cell pellets were resuspended in 5 ml lysis buffer (50 mM sodium phosphate pH 7.8, 200 mMNaCl, 100 mMKCl, 20% glycerol, 10 mMethylene diamine tetraacetic acid [EDTA], 2 mMdithiotreitol [DTT], 1 mMphenylmethane sulfonyl fluoride [PMSF], 50 μg/ml lysozyme, 20 μg/ml DNase I) per

gram pellet weight, freeze-thawed three times on dry ice and at 37°C, and lysed by passing through a French press at 18,000 psi. Cell debris was removed by centrifugation at 6,600 ×g for 15 min. The supernatant was centrifuged at 126,000 ×g for 1 h to collect the membrane fraction and soluble fraction. The soluble fraction was poured onto a NTA histidine-binding column (Sigma) equilibrated with 10 column volumes of lysis buffer. The column was washed with buffers containing increasing concentrations of imidazole to remove non-specific bacterial contaminants, and proteins were eluted with 3 ml elution buffer (20 mM sodium phosphate, 0.5 M NaCl, 0.5 M imidazole, pH 7.3).

The membrane fraction was suspended in 5 ml of membrane lysis buffer (20 mM sodium phosphate, 0.5 M NaCl [pH 7.8], 1% FC-12) per 1 gram pellet and rotated at room temperature for 2 h. The lysates were sonicated intermittently in 30-s bursts to fully resuspend the pellets. The lysates were then clarified by centrifugation at 16,000 ×g for 20 min at 4°C. The clarified supernatants were poured onto a 5-ml bed volume of NTA histidine-binding beads equilibrated with 10 column volumes of binding buffer. Both ends of the column were immediately capped, and the columns were rotated at 4°C overnight. The columns were washed consecutively with 10 ml of 20 mM sodium phosphate, 0.5 M NaCl (pH 7.8), 0.05% FC-12, and 20 and 40 mM imidazole to remove non-specific bacterial contaminants. The proteins were eluted with 3 ml elution buffer (20 mM sodium phosphate, 0.5 M NaCl, 0.5 M imidazole [pH 7.3], and 1% FC-12). The elution buffer was removed from the purified proteins on a PD-10 column equilibrated with phosphate-buffered saline (PBS) with 0.2% FC-12. Fractions of 1 ml each were collected and screened for OD600 readings. The peak fractions were pooled and quantified by the Bradford assay (Bio-Rad, Hercules, CA). The resulting purified recombinants were stored at -80°C.

HIV-1 envelope-mediated cell fusion assay and single-round virus infection assay

HIV-1 Env-mediated fusion was performed by a *Vaccinia*-based reporter assay as previously described [28]. Briefly, target THP-1 cells were infected with *Vaccinia* virus encoding the bacteriophage T7 RNA polymerase. Effector HeLa cells were co-infected with PT7-lacZ *Vaccinia* virus and *Vaccinia* virus encoding either R5 BaLEnv, or the control Unc, an uncleaved HIV-1 Env protein that has its cleavage site mutated and therefore cannot engage in membrane fusion. The UncEnv protein was used to measure the non-specific background in the fusion assay. The target or effector cells were plated in a 96-well plate at 1×10^5 cells per well and treated for 1 h with or without either soluble recombinant T4L-CCR5 or CCL5. After a 1-h incubation at 37°C in a 6% CO_2 incubator, the Env-expressing effector cells were mixed with the target cells at a ratio of 1:1. The cell mixtures were incubated for 2.5 h at 37°C, then lysed, and the substrate chlorophenolred-β-D-galactopyranoside (CPRG) was added. The extent of cell fusion was assayed by measuring the amount of β-galactosidase produced.

We adapted the improved pseudotyping assay developed by He *et al.* (1995) to prepare pseudotyped virus particles. 293T cells were co-transfected with 5 μgPcREV and 20 μg of the envelope-defective luciferase-transducing HIV proviral clone pNL4-3.Luc+env in the presence or absence of 10 μg of HIV-1 BaL–Env expression vectors using standard calcium phosphate (Promega, Madison, WI). Fifteen hours after transfection, 20 mM sodium butyrate and fresh media were added. The supernates were harvested after 48–72 h by centrifugation at 1500 rpm for 5 min, and filtered through a 22-μm filter. The virus stocks were stored at -80°C. Vesicular stomatitis virus G glycoprotein (VSV-G) was used as a positive control to verify the competence of cells with respect to cell fusion. HIV-1 p24 antigen was quantified by enzyme-linked immunosorbent assay (ABL, Inc. Rockville, MD) and normalized to luciferase activity (relative luminescence units per min) by titration of viral supernates from U373 cells. Pseudotyped virus infection assays were performed by incubating 1×10^5CCR5 sorting-positive 3T3.T4 cells transfected withT4L-CCR5 variants, containing 5 μg/ml polybrene mixed with 1 ml of virus stock in a six-well plate. The mixture was incubated for 4–5 h at 37°C in a 5% CO_2 incubator. Following incubation, the cells were washed with 10% FBS, fresh medium was added, and incubation was continued for another 48 h. The cells were harvested, and the luciferase assay was performed using the luciferase assay system as recommended by the manufacturer (Promega, Madison,WI).

Ligandbinding and [35S]GTPγS-binding assays

Chemokine-binding assays were conducted as previously described [29]. Briefly, 48 h after transfection with T4L-fused CCR5 constructs, HEK-293 cells were harvested in PBS containing 0.5% bovine serum albumin and 0.01% sodium azide. Specific binding was performed by incubating 10^6 cells in duplicate with 0.3 nmol/liter [125I]-CCL4 or [125I]-CCL5 (2000 Ci/mmol; PerkinElmer, Massachusetts). Non-specific binding was determined by the addition of 1 mol/liter unlabeled CCL4 or CCL5. After 2 h at 37°C, unbound chemokines were separated from the cells by pelleting them through a 10% sucrose/PBS cushion. Bound ligands were quantified by counting gamma emissions.

Competition binding assays were performed in Minisorb tubes (Nunc) using 0.08 nmol/liter [125I]-MIP-1β or [125I]-MCP-2 (2200Ci/mmol, NEN) as tracer, variable concentrations of competitors (R&D Systems), and 50,000 cells in a final volume of 0.1 ml. Total binding was measured in the absence of competitors, and non-specific binding was measured with a 100-fold excess of unlabeled ligand. Samples were incubated for 90 min at 37°C, then bound tracer was separated by filtration through GF/B filters presoaked in 1% bovine serum albumin (BSA) for [125I]-MIP-1β or 0.3% polyethylenimine (Sigma) for [125I]-MCP-2. Filters were counted in a β-scintillation counter.

The [35S]GTPγS binding assay was carried out as described [30]. Cells were lysed in buffer containing 5 mMTris-HCl, pH 7.5, 5 mM EDTA, and 5 mM EGTA at 4°C. The membrane pellet resulting from a 30,000 ×g centrifugation was resuspended, and aliquots containing 10 μg protein were incubated at 30°C for 1 h in buffer containing 50 mMTris-HCl, pH 7.5, 1 mM EDTA, 5 mM $MgCl_2$, 100 mMNaCl, 40 μM GDP, and 0.5 nM [35S]GTPγS (1,200 Ci/mmol) in the presence or absence of the agonists in a total volume of 100 μl. The reaction was terminated by adding cold PBS and filtered through GF/C filters, which were counted in a liquid scintillation spectrophotometer. Basal binding was determined in the absence of agonists, and non-specific binding was obtained in the presence of 10 μMGTPγS. The percentage of

stimulated [35S]GTPγS binding was calculated as 100 × (cpm_{sample} – $cpm_{nonspecific}$) / (cpm_{basal} – $cpm_{nonspecific}$).

Chemotaxis assays

Chemotaxis assays were performed as previously described [29]. Briefly, for CCL5-mediated chemotaxis, macrophages were suspended in chemotaxis medium [Iscove's Modified Dulbecco's Medium (IMDM)] supplemented with 0.5% BSA at a density of 2×10^6 cells/ml. Commercial CCL5 (100 nM), with or without purified recombinant T4L-CCR5 protein (100 nM each), was suspended in chemotaxis medium. The suspended mixtures (in 0.6 ml) were first added to the wells of a 24-well plate, followed by the placement of a 5-micron pore Transwell membrane to each well (Costar, Corning Incorporated, Acton, MA). The cells were added to the inside of the Transwell membrane at a volume of 0.1 ml (2×10^5 cells). The plates were then capped and incubated for 4 h at 37°C in a 5% CO_2 incubator. After the incubation period, the Transwell membranes were removed from the wells and the migrated cells counted by flow cytometry.

Flow cytometry

HEK-293 cells were transfected with pSC-IRES-GFP-T4l-CCR5 vectors using DOTAP (Roche) and then activated by *Vaccinia* virus infection. Fluorescent-activated cell sorting (GFP-positive) was carried out 16 h after infection, and the level of CCR5 expression was measured by flow cytometry using phycoerythrin (PE)-conjugated 2D7 and PE-conjugated 3A9 monoclonal antibodies. Briefly, after washing, cells were incubated with 1 µg/ml 2D7 or 3A9 at room temperature for 15 min. After washing again, cells were fixed in 1% paraformaldehyde/PBS. The red (CCR5) fluorescence was analyzed with a FACScan flow cytometer (Becton Dickinson, San Jose, CA). Results were expressed as the percentage of PE-positive cells in the GFP-positive fraction. For intracellular staining, a Cytofix/Cytoperm kit from BD Biosciences (San Jose, CA) was used. MDM was pretreated with or without soluble recombinant CCR5-T4L protein for 2 h at 37°C in a 5% CO_2 incubator. After the incubation period, the soluble recombinant protein was removed by washing at least three times using PBS, and the cells were analyzed by flow cytometry.

Gel electrophoresis and western blotting

Fifteen microliters of protein sample were mixed with the same volume of 2× SDS loading buffer and incubated at 37°C before separation by sodium dodecyl sulfate polyacrylamide gel electrophoresis (SDS-PAGE). The transfer was performed at 0.5 A constant current for 1 h in the transfer buffer (1×Tris-Glycine buffer containing 20% methanol, Bio-Rad). The membrane was incubated with mouse monoclonal His-tag antibody at a 1:2000 dilution for 2 h followed by three washes for 5 min each with TBST buffer. Subsequently, the membrane was incubated with goat anti-mouse IgG/M HRP antibody at a dilution of 1:5000 for 1 h. After washing four times for 5 min each with TBST buffer, the blot was developed using ECL Plus western blot detection reagents (GE Healthcare).

RESULTS

PCR-based T4L-CCR5 genes synthesis –Fusion of a T4L to the wild-type CCR5

Genes of T4L-CCR5 structures were synthesized *de novo* from a set of overlapping DNA oligonucleotides using a two-step amplification PCR method. The T4L-CCR5 variants were designed by replacing the first, second, or third intracellular loop, or different C-terminal fragments, of wild-type CCR5 with T4L (Fig1A). These designed genes were generated as PCR fragments (Fig. 1B). Either three or two PCR fragments (depending on the placement of the T4L moiety) were generated using the indicated primer pairs (Supplemental Data 1) from full-length CCR5 and T4 lysozyme. Overlapping primer regions,represented in the same color in Supplemental Data 1, were necessary for the second round of PCR to generate full-length T4L-CCR5 variants. After purification, 50 ng of each first-round PCR product was used as the template in the second round of PCR. Subsequently, we cloned sixsynthesized T4L-CCR5 variants (T4L-CCR5-ICL1, T4L-CCR5-ICL2, T4L-CCR5-ICL3, T4L-CCR5-C352, T4L-CCR5-C333, and T4L-CCR5-C310)into the pET-20b and pSC-IRES-GFP vectors. The pET-20b vectors were used for recombinant protein expression in a bacterial system, and the pSC-IRES-GFP vectors were used for functional analysis.

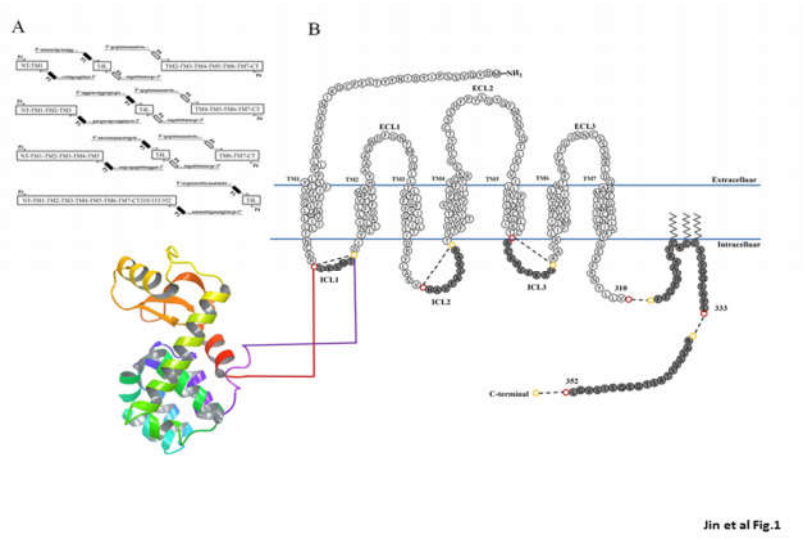

Fig. 1 Overview of the construction ofT4L-fused CCR5 variants. (A) Primer design for the T4L-CCR5 variants. Either three or two fragments (depending on T4L placement) were generated using the indicated primer pairs from full- length CCR5 and T4L (see Supplemental Data S1). Overlapping regions of the same color were necessary for homologous two-step PCR amplification. (B) Design and construction of six T4L-CCR5 variants.

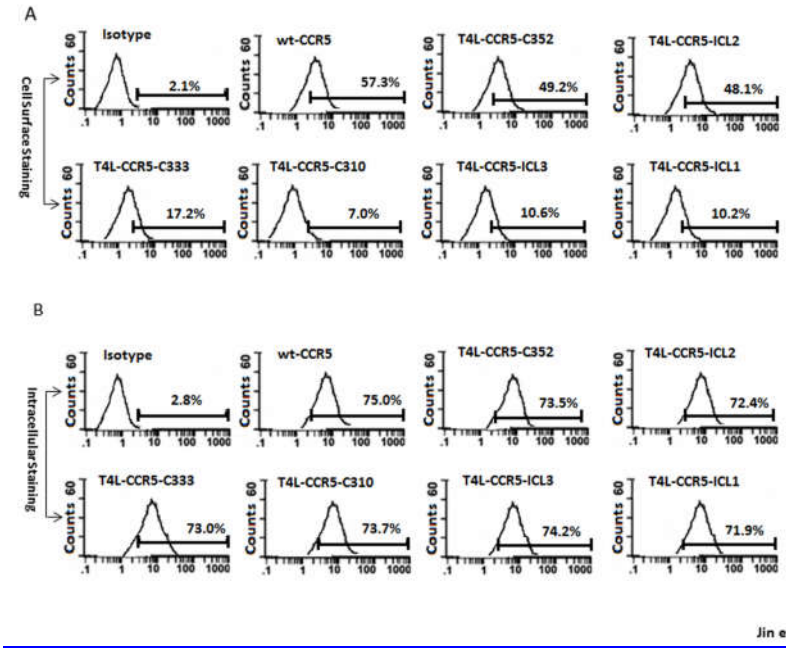

Fig. 2 T4L-CCR5 variants are expressed on the HEK-293 cell surface. Following the transient transfection of HEK-293 cells with T4L-CCR5 variant plasmids or control pSC-IRES-GFP vector, the expression levels of wild-type CCR5 as well as of T4l-CCR5-ICL1, T4L-CCR5-ICL2, T4L-CCR5-ICL3, T4L-CCR5-C310, T4L-CCR5-C333, and T4L-CCR5-C352 were analyzed by fluorescent-activated cell sorting using 2D7-phycoerythrin (PE), a monoclonal antibody mapping to the second extracellular loop of the receptor. Control HEK-293 cells transfected with pSC-IRES-GFP were used as negative control. Immunofluorescent staining of cellsurface CCR5 (A), and a test for intracellular CCR5 after fixing and permeabilizing the cells using a Cytofix/Cytoperm kit from BD Biosciences (B).

Functional expression of T4L-CCR5 constructs on the HEK-293 cell surface

Surface expression was assayed on transiently transfected HEK-293 cells by flow cytometry using the 2D7 PE-conjugated monoclonal antibody, recognizing a conformation-sensitive epitope in the ECL2. Each T4L-CCR5 structure allows simultaneous EGFP expression under the IRES promoter from the same RNA transcript to control transfection efficiency. The results, shown in Fig 2A, were compared between wild-type CCR5-transfected cells and pSC-IRES-GFP vector-transfected cells stained with the same antibody. Wild-type CCR5-transfected cells showed a 27.3-fold increase in mean log fluorescence over negative control (vector-transfected) HEK-293 cells. Variants T4L-CCR5-C352 and T4L-CCR5-ICL2 were expressed on the cell surface and showed 23.4-fold and 22.9-fold increases in mean log fluorescence over the negative control cells, respectively. The T4L-CCR5-C333 variant was also expressed on the cell surface and showed an increase of 8.2-fold over negative control cells. Variants T4L-CCR5-C310, T4L-CCR5-ICL3, and T4L-CCR5-ICL1 were expressed on the cell surface and showed 3.3-, 5.0-, and 4.8-foldincreases in mean log fluorescence, respectively (Fig. 2A). To investigate the relative roles of decreased protein synthesis and export impairment, the subcellular distribution of the receptor variants was analyzed by fixing and permeabilizing the cells using BD Cytofix/Cytoperm buffer. All T4L-CCR5 constructs exhibited nearly the same expression levels as did wild-type CCR5, which exhibited a 27-fold increase in mean log fluorescence over that seen in negative control cells (Fig. 2B). These results suggested that T4L engineering did affect the expression of the receptor on the cell surface.

T4L-CCR5 variants act as functional GPCRs in terms of receptor signaling, internalization, and desensitization in HEK-293 cells

CCR5 binds to a number of ligands, including CCL3 (MIP-1α), CCL4 (MIP-1β), and CCL5 (regulated on activation, normal T cell expressed and secreted; RANTES). To test whether T4L engineering would interfere with the protein's ability to function as a chemokine receptor, HEK-293 cells transiently transfected with T4L-CCR5 plasmids were tested for specific binding of ^{125}I-CCL4. These variants exhibited different chemokine binding affinities and could be categorized into two different groups. The first group included T4L-CCR5-ICL2, T4L-CCR5-C352, and T4L-CCR5-C333, which displayed ^{125}I-CCL4 binding comparable to that of wild-type CCR5 (Fig 3A). All these variants exhibited similar binding affinities for CCL4, with EC_{50}values of 0.061±0.004 nM, 0.072±0.006nM and 0.371±0.025nM, respectively, compared with 0.033±0.004nMfor wild-type CCR5. The EC_{50} values of the other group, which included T4L-CCR5-ICL1, T4L-CCR5-ICL3, and T4L-CCR5-C310, were significantly reduced to 0.471±0.022nM, 0.489±0.024nM, and 0.556±0.021nM, respectively (Fig. 3A). Using a [^{35}S]GTPγS binding-based assay, we further investigated the responses of T4L-CCR5 variants to chemokine CCL4 stimulation. T4L-CCR5-ICL2, T4L-CCR5-C352, and T4L-CCR5-C333 maintained the ability to activate G-proteins (EC_{50} values: 2.100±0.326 nM, 2.132±0.280 nM, and 1.628±0.555nM). This ability was reduced for T4L-CCR5-ICL1 (EC_{50}=5.455±0.511 nM) and T4L-CCR5-ICL3 (EC_{50}=6.987±0.501 nM) and was significantly decreased for T4L-CCR5-C310 (EC_{50}=28.88±6.75 nM) (Fig 3B). Pretreatment with pertussis toxin (PTX) abolished agonist-stimulated G protein activation, indicating that T4L-

constructs were functionally coupled to PTX-sensitive G-proteins (Fig. 3C).

Exposure of CCR5-expressing membranes to TAK-779 or Maraviroc (MVC) resulted in a dose-dependent decrease in [^{35}S]GTPγS binding (Fig. 3F-G).These variants exhibited the differential effects of CCR5 inhibitors on basal [35S]GTPγS binding and could be categorized into two different groups, indicating that membranes expressing T4L-CCR5-ICL1, T4L-CCR5-ICL3, and T4L-CCR5-C310 are more sensitive to CCR5 agonists. Our results demonstrate that these T4L-CCR5 variants have different abilities to activate G-proteins. The ability of T4L-CCR5-ICL2, T4L-CCR5-C352, and T4L-CCR5-C333 to activate G-proteins was higher than that of T4L-CCR5-ICL1, T4L-CCR5-ICL3, and T4L-CCR5-C310.The data also suggest that MVC and TAK-779 stabilize different conformations of T4L-CCR5 variants. In particular, MVC was less efficient at reducing basal [35S]GTPγS binding to T4L-CCR5 expressing membranes than TAK-779. Together, our data indicate that T4L-CCR5-ICL1, T4L-CCR5-ICL3, and T4L-CCR5-C310 mutant receptors are defective in the ability to activate G-proteins.

responsiveness of the wtCCR5 and T4L-CCR5 constructs was significantly reduced followingpreincubation with the agonist of the corresponding receptor RANTES, suggesting that T4 lysozyme engineering does not affect the feedback regulation of CCR5. Treatment with the protein kinase C (PKC) activator phorbolmyristate acetate, which mimicked agonist pretreatment, had no significant effect on basal adenylyl cyclase activity, indicating that PKC recognizes and regulates wtCCR5 and T4L-CCR5 constructs in these cells. Furthermore, co-expression of the wtCCR5 and T4L-CCR5 constructs with either GRKs (2 or 5) or β-arrestins (1 or 2) significantly attenuated the receptor-mediated inhibition of cAMP (Fig. 3D-E).

T4L-CCR5 constructs and HIV-1 co-receptor function

To determine whether T4L-CCR5 constructs have HIV co-receptor function, we first measured fusion efficiency using an Env-mediated cell-cell fusion assay. 3T3.T4 cells, transfected with T4L-CCR5 variant plasmids and infected with *Vaccinia* virus-encoded T7 RNA polymerase, were used

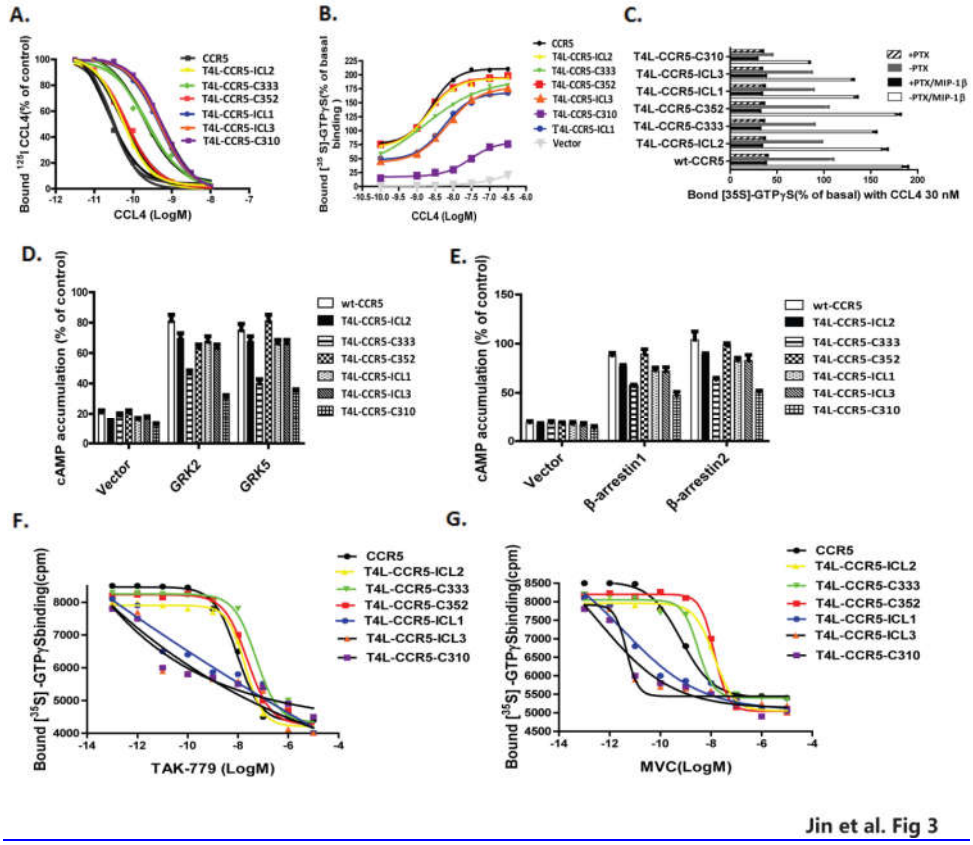

Fig. 3.Cellular responses mediated byT4L-fused CCR5 chemokine receptor. (A) Competitive binding of [^{125}I] CCL4 to HEK-293 cells transfected with T4L-CCR5 variants using 0.1 nmol/liter ^{125}I CCL4 as tracer. HEK-293 cells transfected with wild-type CCR5 and T4L-CCR5 variants were tested for their ability to bind CCL4. Non-specific binding was determined using 1 μmol/liter unlabeled CCL4 as competitor. (B) CCL4-induced [^{35}S]GTPγS binding to membranes from HEK 293T cells transfected with vector, wt-CCR5, or different T4L-CCR5 variants. Membranes were incubated in assay buffer containing 0.1 nM [^{35}S]GTPγS, 1 μM GDP, and 3 mM $MgCl_2$, and the indicated concentrations of CCL4. The data were normalized for basal binding to membranes from cells transfected with vector only (0%). (C) Functional coupling of the T4L-CCR5 chemokine receptors to PTX-sensitive G-proteins. HEK-293 cells transiently expressing wild-type CCR5 or T4L-CCR5 variants were pretreated with or without 30 nM CCL4 or 100 ng/ml PTX and cultured for 15 h. D) Functional interaction of the T4L-CCR5 chemokine receptors with receptor kinases. HEK-293 cells were transiently transfected with wild-type CCR5 and T4L-CCR5 variants alone (control), or co-transfected with GRK2 and GRK5 (D) or with β-arrestin 1, or β-arrestin 2 (E). Inhibition of the cAMP accumulation induced by 30 nM CCL5 was determined. Untreated forskolin-stimulated cAMP levels were in the range of 116±11 pmol/mg protein. Transfection efficiency was measured based on GFP expression. The data presented are averages and error ranges of three separate experiments performed in duplicate. Dose-dependent effects of TAK-779 (F) or MVC (G) on basal [^{35}S]GTPγS binding to membranes expressing wild-type CCR5 or T4L-CCR5 variants. All experiments are representative of at least three independent experiments. Data points represent the mean±S.E. of triplicate determinations.

We also investigated T4L-CCR5 receptor desensitization and interaction with receptor kinases and arrestins using the cAMP assay. As shown in Supplemental Data 2, the

as target cells. Effector HeLa cells were co-infected with recombinant *Vaccinia* virus encoding the T7-lacZ reporter gene and *Vaccinia* virus encoding the R5 BaL Envelope. The

infected target cells were mixed with Env-expressing cells and the extent of Env-mediated cell fusion was measured by β-gal production. The expression of the T4L-CCR5-ICL2 and T4L-CCR5-C352 variants in 3T3.T4 cells resulted in efficient fusion with the HeLa-R5-BaL Env cells. The β-gal signals obtained with these two variants were 82% and 88% that of wild-type CCR5. Cells expressing the T4L-CCR5-ICL1, T4L-CCR5-ICL3, and T4L-CCR5-C310 variants produced a very low fusion signals (12%, 10%, and 8%, respectively) in response to HeLa cells expressing R5-BaL Env. The fusion efficiency of cells expressing the T4L-CCR5-C333 variant was markedly decreased (only 25% that of wild-type CCR5) (Fig 4A).

weremore functional in terms of HIV co-receptor function rather than cell surface CCR5 expression.

T4L-CCR5 fusion protein expression and purification using an Escherichia coli expression system

Large-scale expression was successfully performed in 5-L shaking flasks containing about 1 L (LB) culture media. Cell pellets were stable at –70°C for at least 6 months. Membranes containing T4L-CCR5 variants were isolated from these cell pellets by several homogenization and centrifugation steps. The stability of the resulting membrane preparation stored at –70°C was checked based on recognition by specific CCR5 or His-tag antibodies.

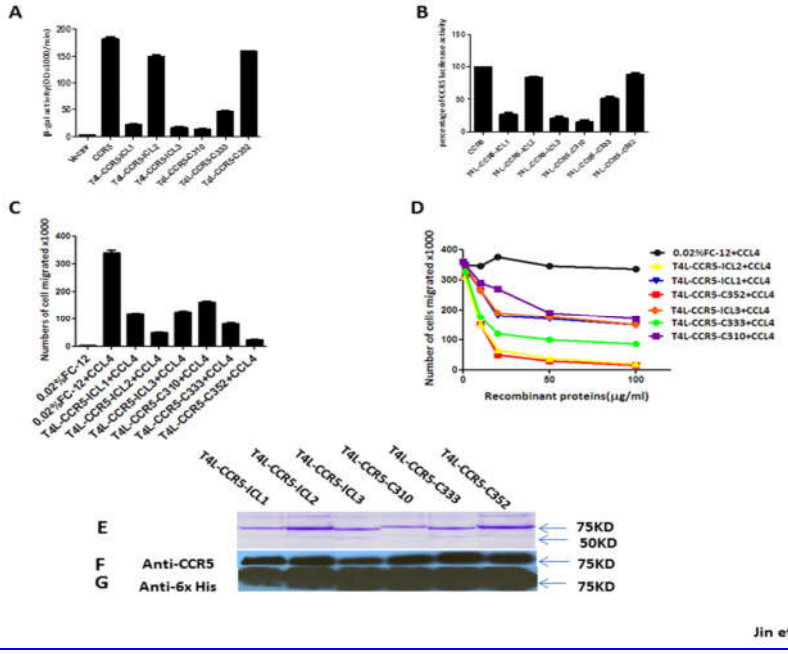

Fig. 4. **T4L-CCR5-C352 and T4L-CCR5-ICL2 show HIV-1 co-receptor function, and recombinant T4L-CCR5 variant proteins show blocking effects in a CCL4-induced migration assay. (**A) Co-receptor activities of T4l-CCR5 variants relative to that of wild-type CCR5 were determined by a cell-cell fusion assay. The assays were performed using 3T3.T4 cells transiently transfected with variants of T4 l-CCR5 and expressing CD4 and T7 RNA polymerase, and also using HeLa cells expressing the HIV R5 envelope (Ba-L) and expressing the PT7-lacZ reporter genes. A mixture of both 3T3.T4 and HeLa cells were incubated at 37°C, and the extent of fusion was quantified by measuring the amount of β-galactosidase produced. The results are representative of at least three different experiments performed in duplicate. 3T3.T4 cells transfected with the pSC-IRES-GFP vector were used as negative controls. (B) 3T3.T4 cells transfected with wild-type CCR5 and T4l-CCR5 variants were infected with luciferase reporter virus pseudotyped with Ba-L. Forty-eight hours later, luciferase activity in active and control 3T3.T4 cell lysates was measured. Results are shown as the percentages of luciferase activity in wild-type CCR5 transfected cells (means of three independent wells±SD). CCL4-induced chemotactic activity was blocked by adding 100 μg/ml purified recombinant T4L-CCR5 protein. The same volume of PBS was used as a negative control. Chemotaxis assays were performed using ghost hi5 cells (C). The chemotactic activity of the chemokine CCL4 was examined in the presence of increasing concentrations of purified recombinant T4L-CCR5 proteins (D) in a two-chamber chemotaxis assay. Error bars indicate standard deviations from mean values obtained from triplicate measurements. These data are representative of three experiments done at different times with different chemokine purification sets. (E-G) SDS-PAGE detection and western blot identification of purified recombinant T4L-CCR5 proteins. All samples were prepared by mixing 15 μl of dialyzed elution sample with 15 μl of 2× sample buffer and incubating at 30°C for 15 minutes prior to loading on a 10% SDS-PAGE gel. Proteins were stained by Coomassie Brilliant blue R-250 (E) or probed by rabbit anti-human CCR5 polyclonal antibody (NT) (F) or mouse anti-6× His monoclonal antibody (G).

To further test whether T4L-CCR5 variants influence HIV-1 entry, single-round infection assays were performed with pseudotyped viral particles, which were generated with an envelope-defective luciferase reporter HIV-1 provirus complemented with the X4R5 primary HIV-1 89.6 envelope, using cells that sorted positive for CCR5. Luciferase activity in cells transfected with the T4L-CCR5-ICL2 (80%) and T4L-CCR5-C352 (82%) variants was comparable to that in wild-type-transfected cells, but it was lower in cells transfected with the T4L-ICL1 (30%), T4L-CCR5-ICL3 (23%), T4L-CCR5-C310 (20%), and T4L-CCR5-C333 (48%) variants (Fig 4B). These results suggest that two engineered T4 lysozyme variants, C-terminal-fused T4L (T4L-CCR5-C352) and second intracellular loop-fused T4L (T4L-CCR5-ICL2),

For the solubilization of membrane proteins, the detergents Cymal-5, DDM, FosCholine-12, Brij 58, and Brij78 were tested. In agreement with previous reports, FosCholine-12 (FC-12) gave good results for protein solubilization and stabilization. Therefore, FC-12 was used for all further experiments. Washed cell membrane fractions were dissolved in the solubilization buffer (50 mM sodium phosphate pH 7.8, 200 mMNaCl, 10% glycerol, 2% FC-12, and protease inhibitor) and subjected to ultracentrifugation at 100,000 ×g for 1 hour to remove non-solubilized proteins. The supernates were loaded on a Hi-Trap Chelating HP 5-ml column, which was charged with chelated Ni^{2+} and equilibrated with binding buffer (50 mM sodium phosphate pH 7.8, 200 mMNaCl, 100 mMKCl, 0.05% FC-12, 5 mM imidazole) for the first step of

purification. After being washed with 15 column volumes of washing buffer (50 mM sodium phosphate pH 7.8, 200 mMNaCl, 100 mMKCl, 0.05% FC-12, 15 mM imidazole), the target proteins were eluted with 10 ml elution buffer (50 mM sodium phosphate pH 7.8, 200 mMNaCl, 100 mMKCl, 0.05% FC-12, 400 mM imidazole).

All the protein fractions in the purification of T4L-CCR5 variants were identified using western blot detection, using mouse anti-human CCR5 monoclonal (NT) and anti-His monoclonal (anti-6× His) antibodies. The eluates from the Ni^{2+}chelating column purification of T4L-CCR5 variants were also identified using thethe same antibodies (Figure 4F-G). The final yields were 10 mg purified recombinant T4L-CCR5-ICL3 protein from 1 liter bacterial growing media. For other variants, 1 mg protein was collected from 1 liter media. However, in addition to the 85-kDa band, one smaller fragment, except in the case of T4L-CCR5-C310, showed a positive reaction with the anti-His monoclonal antibody. We speculated that this might bea cleavage product from the C-terminus of the T4L-CCR5 variants that has an apparent molecular weight of 55 kDa (Figure 4E).

Characterization of detergent-solubilized purified T4L-CCR5 proteins

To characterize the functions of the purified T4L-CCR5 proteins, we first measured specific CCL4 binding for all T4L-CCR5 constructs, using an *in vitro* chemotaxis assay.

We used cells from a ghost Hi5 cell line as the target cells. The efficiency of induced migration was compared among different amounts of purified T4L-CCR5 variant proteins mixed with 100 μM commercial CCL4 protein. Chemotactic activities significantly decreased upon the addition of 100 μM of recombinant T4L-CCR5-ICL2, T4L-CCR5-C352, and T4L-CCR5-C333 proteins, but only slightly decreased upon the addition of 100 μM each of recombinant T4L-CCR5-ICL1, T4L-CCR5-ICL3, and T4L-CCR5-C310 proteins (Figure 4C-D).

To further confirm the HIV co-receptor function of the purified recombinant T4L-CCR5 variant proteins, we tested their inhibitory activities in an HIV-1 Env-mediated cell-cell fusion assay. A dose-response analysis was performed for each of the T4L-CCR5 variants, which waspreincubated with 0.01nM of soluble CD4 and effector HeLa cells co-infected with recombinant *Vaccinia* virus encoding the R5 Ba-L Env or X4 LavEnv proteins (Figure 5A-B). The results show that 20 ng/ml of the T4L-CCR5-C352 variant caused ~50% inhibition of cell-cell fusion. Increasing the concentration of recombinant T4L-CCR5-C352 protein resulted in a dose-dependent inhibitory effect. Doubling of the number of target cells expressing positive CD4 and CCR5 molecules reduced the inhibitory activity (Figure 5C-D).The X4 LavEnv protein was used as a negative control. None of the purified recombinant T4L-CCR5 variant proteins showed any inhibition of X4 Env-mediated fusion (data not shown).

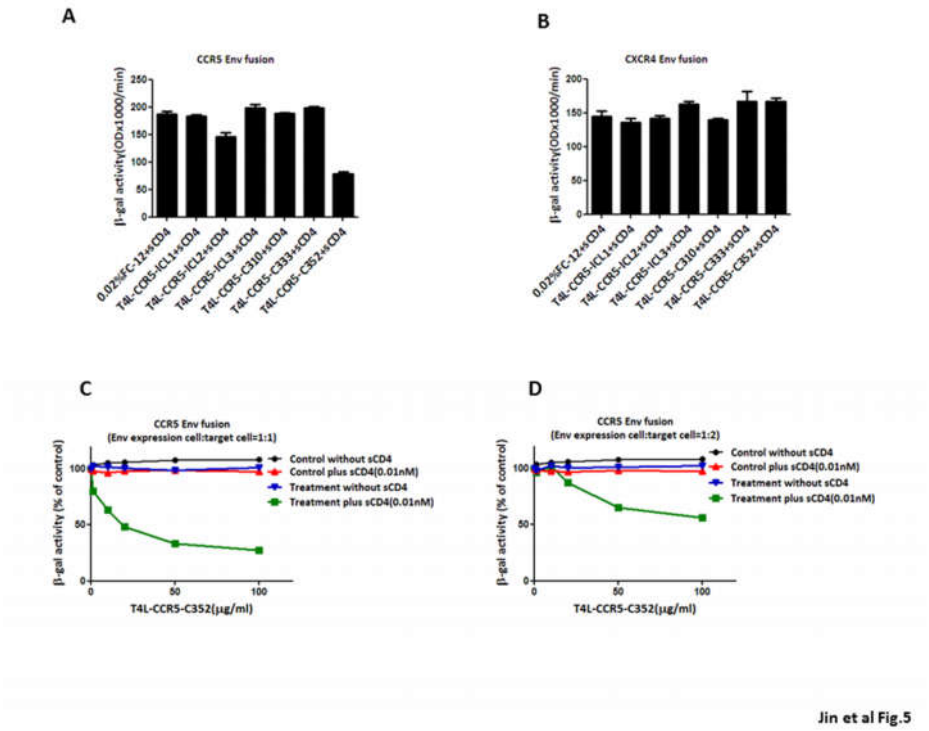

Fig. 5.Purified recombinant T4L-CCR5-C352 exhibits a competitive blocking effect in R5 Env-mediated cell-cell fusion. (A) 3T3.T4.R5 cells expressing CD4, CCR5, and T7 RNA polymerase and HeLa cells expressing the HIV R5 envelop (Ba-L) and PT7-lacZ reporter genes were mixed following pretreatment of the HeLa cells with soluble CD4 plus 100 μg/ml each of purified recombinant T4L-CCR5 protein, and incubated at 37°C. The extent of fusion was quantified by measuring the amount of β-galactosidase produced. The same volume of PBS was used as a negative control. (B) T4L-CCR5-C352 shows no inhibitory effect on CXCR4 Env-mediated cell-cell fusion. (C) Dose-dependent effect of T4L-CCR5-C352 on cell-cell fusion between 3T3.T4.R5 cells expressing CD4, CCR5, and T7 RNA polymerase, and HeLa cells expressing the HIV R5 envelope (Ba-L) and PT7-lacZ reporter genes. Prior to mixing together 0.1×10^6 of each cell type, the HeLa cells were pretreated with soluble CD4 plus different concentrations (0, 5, 10, 25, 50, and 100 μg/ml) of T4L-CCR5-C352 at 37°C for 1 h. (D) The blocking effect decreased following the mixing of 0.2×10^6 3T3.T4.R5 cells with 0.1×10^6 HeLa cells. We used a low concentration of sCD4: 0.01 nM. In Figures 5A and 5B, as well as Figures 5C and 5D, all treatment conditions included 0.01 nM sCD4. The negative control, which is PBS only, was treated with 0.02% detergent FC-12 PBS solution plus 0.01 nM sCD4. Furthermore, "treated" samples were treated with T4L-CCR5-C352 in 0.02% FC-12 PBS solution plus 0.01 nM sCD4. The results are representative of at least three different experiments performed in duplicate.

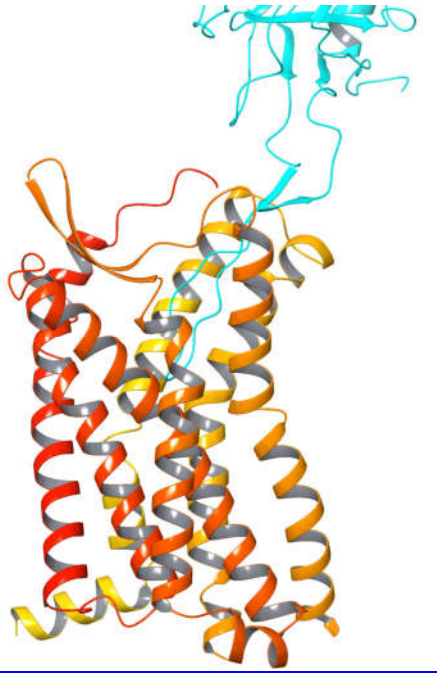

Fig. 6 A structural model of the CCR5-gp120 complex. This complex model was generated based on the crystal structures of CCR5 (PDB ID: 4MBS) and gp120 (PDB ID:3ODU) using the Maestro 9.3 suite from Schrödinger®.

Different roles of T4 lysozyme-engineered CCR5 in HIV-1 co-receptor function and ligand-binding function

The role of co-receptor signaling in HIV disease has not been clearly defined. Our results showed that T4L-CCR5-ICL2 and T4LCCR5-C352 retained sufficient HIV-1 co-receptor function. In contrast, although the surface expression levels of T4L-CCR5-C310, T4L-CCR5-ICL3, and T4L-CCR5-ICL1 were maintained, HIV-1 co-receptor function was not observed in these variants. To explore the potential structural effects of these fused T4L moieties on CCR5, we constructed a CCR5-gp120 complex model based on the crystal structures of CCR5 (PDB ID: 4MBS)1 and gp120 (PDB ID:3ODU)2. The complex model was built by manually docking gp120 into the transmembrane pocket near the extracellular side of CCR5 using the Maestro 9.3 suite from Schrödinger® (Fig. 6). From a structural point of view, because both gp120 and the substrate of CCR5 bind to CCR5 through their corresponding binding sites that are located on the extracellular side of the receptor, the fused-T4L is unlikely to have a direct effect on either the substrate binding or co-receptor functions of CCR5. This is consistent with T4L replacement at the second intracellular loop. On the other hand, the defective co-receptor function caused by replacements at other positions indicated that those T4Lfusions might indirectly change the conformation or dynamics of the N-terminus or the extracellular loops of CCR5, where they interact with the gp120. Interestingly, all T4L-CCR5 variants preserved their chemokine binding function, suggesting there are different pathways for HIV-1 co-receptor function and ligand binding in CCR5, which is consistent with the two-site CCR5 model [6].

DISCUSSION

The aim of this study was to investigate biological functional changes in different T4 lysozyme-engineered CCR5 variants. It has been reported that the ICL3 is usually chosen as the site for the CCR5 fusion protein. However, we found that T4L-CCR5-ICL3 not only exhibited lower cell surface expression but also lacked HIV-1 co-receptor function *in vitro*, as did T4L-CXCR4-ICL3. In order to identify functional variants, we inserted T4L into one of either the three intracellular loops or at different regions of the C-tail to build six different T4L-CCR5 variants. Compared to WT-CCR5, all these variants showed augmented stability and increased yields in an *E. coli* system. We substituted T4L (aa: 2–161) for ICL1 (aa: 61–65, "LKSMT"); ICL2 (aa: 132–139,"HAVFALKA"); ICL3 (aa: 223–230, "RCRNEKKR"); C310 (aa: 311–352); C333 (aa: 334–350); and C352 (no stop codon). Our results demonstrate that the fusion of T4L into the C-terminal region (T4L-CCR5-C352) and the second intracellular loop (T4L-CCR5-ICL2) did not affect HIV co-receptor function in mammalian cell systems. In contrast, replacement with T4L in the first and third intracellular loops (T4L-CCR5-ICL1, T4L-CCR5-ICL3) of wild-type CCR5 almost completely eliminated HIV co-receptor function but had no significant effect on chemokine receptor function. The loss of HIV co-receptor function indicates that the insertion of T4L at the first or the third intracellular loop of CCR5 may indirectly affect its interactions with gp120 at the N-terminal and/or the extracellular regions. Because a conserved Asp-Arg-Tyr (DRY) motif in the second intracellular loop of CCR5 is involved in governing receptor conformation and G protein coupling [31], we replaced the HAVFALKA sequence with T4L to avoid interrupting this conserved motif.

Although variants containing a C-terminal truncation of the cytoplasmic tail of CCR5 (T4L-CCR5-C333 and T4L-CCR5-C310) retained ligand-binding activities, we were unable to recover any tail-less T4L-CCR5 fusions that retained HIV co-receptor function. Only recombinant T4L-CCR5-ICL2 and T4L-CCR5-C352 proteinswere able significantly block HIV Env-mediated cell-cell fusion. However, these inhibitory effects likely depend on soluble CD4, which demonstrates that CD4 binding may trigger the formationof an activated intermediate that is competent for bindingto recombinant CCR5 variants. The loss of co-receptor function in variants with a truncated C-terminal domain suggests that the CCR5 C-terminus is also important for CCR5 binding with gp120 and soluble CD4. These observations are consistent with reported data in the literature showing that the C-terminal serine residues of CCR5 regulate receptor signaling and internalization [32,33].

We also present a bacterial system to express large amounts of CCR5 by fusion with the T4 lysozyme. Inserting T4L into the third intracellular loop can yield up to 10 mg of purified protein per liter of bacterial culture, a 10-fold increase in yield when compared to other T4L-CCR5 variants. This is in agreement with previous reports stating that fusion of the third intracellular loop of GPCRs to T4L is a successful strategy for obtaining well-diffracting crystals of these receptors [34, 35]. However, the insertion of T4L into the third intracellular loop of CCR5 does not retain HIV co-receptor activity either in mammalian cells or in recombinant protein purified from *E.coli*. In contrast, insertion of T4L into the second intracellular loop of CCR5 retains 80% HIV co-receptor function compared to wild-type CCR5 in mammalian cells. However, we did not observe this reduction when using

T4L-CCR5-ICL2 recombinant protein in HIV Env-mediated cell-cell fusion.

To date, no recombinant receptor-T4L fusion protein purified from *E. coli* has been reported to act as an HIV co-receptor. The purified T4L-CCR5-C352 variant shows high binding affinity with HIV R5 gp120-expressing cells and soluble CD4 *in vitro,* and could therefore reduce the number of CD4 and CCR5 double-positive target cells fused with Env-expressing cells. This reduction effect was significantly decreased when the number of target cells or the amount of CCR5 expressed on the target cell surface was increased. This evidence strongly suggests that the recombinant T4L-CCR5-C352 protein functions as a competitive inhibitor to wild-type CCR5, demonstrating its potential use as an HIV infection inhibitor. In another study that has been submitted for publication, we found that the soluble recombinant T4L-CCR5-C352 (also named CCR5-T4L) protein slightly promoted HIV infection at low concentrations and inhibited infection at high concentrations [36]. We also demonstrated that a high concentration of soluble recombinant CCR5-T4L had significant antiviral effects in THP-1 cell lines, primary human macrophages, and PBMCs from different donors. Our results suggest that the solubilized T4L-CCR5-C352 variant might be used as an inhibitor of HIV-1 infection.

It remains to be seen whether the insertion of T4L into CCR5 will provide sufficient stabilization to enhance crystallization. However, we anticipate that the developed protocols and knowledge of T4L-CCR5 variant functions will be useful in future crystallization studies of CCR5.

Acknowledgments

We acknowledge the help of the core facility at the Texas Tech University Health Sciences Center, El Paso, for providing DNA sequencing data. We thank Yao Juan for outstanding technical assistance. This study was supported by a grant from the National Natural Science foundation of China (#30870125), and by a grant from theJiangsu Province Natural Science foundation (# SBK201402229), both to Q.J.

Competing Interests

The authors declare that they have no competing interests.

Author Contributions

Q.J., Q.N., and X.J. conceived and designed the experiments; Q.J., Q.N., H.C., L.Z., and H.W. performed the experiments; X.W., Q.X.,G.L.,X.Y.,L.J., and Q.J. analyzed the data; W.Z. contributed reagents, materials, and/or analysis tools; Q.N., Q.J., and X.J. wrote the paper.

References

1. Kooistra AJ, Leurs R, de Esch IJ, *et al*.From three-dimensional GPCR structure to rational ligand discovery.Adv Exp Med Biol. 2014;796:129-57.
2. Rasmussen SG, Choi HJ, Rosenbaum DM, *et al*.Crystal structure of the human beta2 adrenergic G-protein-coupled receptor.Nature. 2007 Nov 15;450(7168):383-7.
3. Rosenbaum DM, Cherezov V, Hanson MA, *et al*.GPCR engineering yields high-resolution structural insights into beta2-adrenergic receptor function.Science. 2007 Nov 23;318(5854):1266-73.
4. Lebon G, Warne T, Edwards PC, *et al*. Agonist-bound adenosine A2A receptor structures reveal common features of GPCR activation.Nature. 2011 May 18;474(7352):521-5..
5. Chien EY, Liu W, Zhao Q, *et al*. Structure of the human dopamine D3 receptor in complex with a D2/D3 selective antagonist. Science. 2010 Nov 19;330(6007):1091-5.
6. Wu B, Chien EY, Mol CD, *et al*.Structures of the CXCR4 chemokine GPCR with small-molecule and cyclic peptide antagonists.Science. 2010 Nov 19;330(6007):1066-71.
7. Shimamura T, Shiroishi M, Weyand S, *et al*.Structure of the human histamine H1 receptor complex with doxepin.Nature. 2011 Jun 22;475(7354):65-70.
8. Hanson MA, Roth CB, Jo E, *et al*. Crystal structure of a lipid G protein-coupled receptor.Science. 2012 Feb 17;335(6070):851-5.
9. Haga K, Kruse AC, Asada H, *et al*.Structure of the human M2 muscarinic acetylcholine receptor bound to an antagonist.Nature. 2012 Jan 25;482(7386):547-51.
10. Kruse AC, Hu J, Pan AC, Arlow DH, Rosenbaum DM, Rosemond E, Green HF, Liu T, Chae PS, Dror RO, Shaw DE, Weis WI, Wess J, Kobilka BK.(2012).Structure and dynamics of the M3 muscarinic acetylcholine receptor. Nature. 2012 Feb 22;482(7386):552-6. doi: 10.1038/nature10867.
11. Granier S, Manglik A, Kruse AC, *et al*. Structure of the d-opioid receptor bound to naltrindole.Nature. 2012 May 16;485(7398):400-4.
12. Manglik A, Kruse AC, Kobilka TS, *et al*. Crystal structure of the μ-opioid receptor bound to a morphinan antagonist.Nature. 2012 Mar 21;485(7398):321-6.
13. Wu H, Wacker D, Mileni M,*et al*. Structure of the human κ-opioid receptor in complex with JDTic. Nature 2012; 485 (7398): 327–32.
14. Aiamkitsumrit B, Dampier W, Antell G, *et al*. Bioinformatic Analysis of HIV-1 Entry and Pathogenesis.Curr HIV Res. 2014 May; 12(2):132-61.
15. Henrich TJ, Kuritzkes DR.HIV-1 entry inhibitors: recent development and clinical use.Curr Opin Virol. 2013 Feb;3(1):51-7.
16. Klasse PJ.The molecular basis of HIV entry. Cell Microbiol. 2012 Aug;14(8):1183-92.
17. Huang, Y., Paxton, W.A., Wolinsky, S.M.,*et al*. The role of a mutant CCR5 allele in HIV-1 transmission and disease progression. Nat. Med.1996; 2:1240-1243.
18. Liu, R., Paxton, W.A., Choe, S.,*et al*. Homozygous defect in HIV-1 coreceptor accounts for resistance of some multiply-exposed individuals to HIV-1 infection. Cell,1996; 86: 367-377.
19. Samson, M., Libert, F., Doranz, B.J.,*et al*. Resistance to HIV-1 infection in caucasian individuals bearing mutant alleles of the CCR5 chemokine receptor gene. Nature,1996; 382:722-725.
20. FDA notifications. FDA notifications. Maraviroc approved as a CCR5 co-receptor antagonistAIDS Alert. 2007 Sep;22(9):103.
21. Arumugam K, Crouzy S, Chevigne A, *et al*. Structure prediction of GPCRs using piecewise homologs and application to the human CCR5 chemokine receptor:

validation through agonist and antagonist docking.*J Biomol Struct Dyn*. 2014;32(8):1274-89.
22. Bozek K, Lengauer T, Sierra S, *et al*.Analysis of physicochemical and structural properties determining HIV-1 coreceptor usage.PLoS Comput Biol. 2013;9(3):e1002977.
23. Nisius L, Rogowski M, Vangelista L, *et al*. Large-scale expression and purification of the major HIV-1 coreceptor CCR5 and characterization of its interaction with RANTES.Protein Expr Purif. 2008 Oct;61(2):155-62.
24. Ren H, Yu D, Ge B, *et al*. High-level production, solubilization and purification of synthetic human GPCR chemokine receptors CCR5, CCR3, CXCR4 and CX3CR1.PLoS One. 2009;4(2):e4509.
25. Wiktor M, Morin S, Sass HJ, *et al*. Biophysical and structural investigation of bacterially expressed and engineered CCR5, a G protein-coupled receptor.*J Biomol NMR*. 2013 Jan;55(1):79-95..
26. Tan Q, Zhu Y, Li J, *et al*. Structure of the CCR5 chemokine receptor-HIV entry inhibitor maraviroc complex.Science. 2013 Sep 20;341(6152):1387-90.
27. Altenburg JD, Broxmeyer HE, Jin Q, *et al*.A naturally occurring splice variant of CXCL12/stromal cell-derived factor 1 is a potent human immunodeficiency virus type 1 inhibitor with weak chemotaxis and cell survival activities.J Virol. 2007 Aug;81(15):8140-8.
28. Jin Q, Altenburg JD, Hossain MM,*et al*. Role for the conserved N-terminal cysteines in the anti-chemokine activities by the chemokine-like protein MC148R1 encoded by Molluscum contagiosum virus.Virology. 2011 Sep 1;417(2):449-56.
29. Altenburg JD, Jin Q, Alkhatib B, *et al*.The potent anti-HIV activity of CXCL12gamma correlates with efficient CXCR4 binding and internalization.*J Virol*. 2010 Mar;84(5):2563-72.
30. Ferrer M, Kolodin GD, Zuck P, *et al*. A fully automated [35S]GTPgammaS scintillation proximity assay for the high-throughput screening of Gi-linked G protein-coupled receptors.Assay Drug Dev Technol. 2003 Apr;1(2):261-73.
31. Lagane B1, Ballet S, Planchenault T, *et al*. Mutation of the DRY motif reveals different structural requirements for the CC chemokine receptor 5-mediated signaling and receptor endocytosis.Mol Pharmacol. 2005 Jun;67(6):1966-76.
32. Venkatesan S, Petrovic A, Locati M, *et al*.A membrane-proximal basic domain and cysteine cluster in the C-terminal tail of CCR5 constitute a bipartite motif critical for cell surface expression.*J Biol Chem*. 2001 Oct 26;276(43):40133-45.
33. Kraft K, Olbrich H, Majoul I,*et al*. Characterization of sequence determinants within the carboxyl-terminal domain of chemokine receptor CCR5 that regulate signaling and receptor internalization.*J Biol Chem*. 2001 Sep 14;276(37):34408-18.
34. Wang X, Cui Y, Wang J.T4-lysozyme fusion for the production of human formyl peptide receptors for structural determination.Appl Biochem Biotechnol. 2014 Mar;172(5):2571-81.
35. Zou Y, Weis WI, Kobilka BK.N-terminal T4 lysozyme fusion facilitates crystallization of a G protein coupled receptor.PLoS One. 2012;7(10):e46039.
36. Jin Q, Chen H, Wang X, Zhao L, Xu Q, Wang H, Li G, Yang X, Ma H, Wu H, Ji X。 The Effects of the Recombinant CCR5 T4 Lysozyme Fusion Protein on HIV-1 Infection.PLoS One. 2015 Jul 8;10(7):e0131894.

****